ORIGINAL CONTRIBUTION

Mechanism of nonthermal induction of apoptosis by high-intensity focused electromagnetic procedure: Biochemical investigation in a porcine model

Yael Halaas MD[1] [iD] | Jan Bernardy MVDr[2]

[1]Facial Plastic and Reconstructive Surgery, New York, NY, USA

[2]Veterinary Research Institute Brno, Brno, Czech Republic

Correspondence
Yael Halaas, Facial Plastic and Reconstructive Surgery, New York, NY, USA.
Email: yaelpt@yahoo.com

Abstract

Background: Multiple studies have reported adipose tissue reduction after the application of the High-Intensity Focused Electromagnetic (HIFEM) field technology, yet cellular level evidence of the mechanisms has remained scarce.

Objectives: This study aims to verify or refute previous single-study histological evidence and further investigates the proposed mechanism of apoptotic induction.

Methods: The thigh of two Large White pigs was treated with HIFEM for 30 minutes. Fat punch biopsies were collected from the application area before, immediately after, and 8 hours post-treatment. Control samples were taken from the abdomen immediately after and 8 hours post-treatment. Samples were analyzed for pro-apoptotic DNA markers (BAX, BCL-2, TXNIP, MMP9, TNF-α), the levels of free fatty acids (FFA), and the pH levels of the adipose tissue.

Results: The levels of FFA in the treated adipose tissue increased on average by 127.1% immediately post-treatment and by 134.1% 8 hours post-treatment, indicating a rapid breakdown of lipids. The average recorded adipose pH changed from 7.30 ± 0.12 at baseline to 6.60 ± 0.07 immediately post-treatment ($P = .001$) and to 7.19 ± 0.12 8 hours post-treatment. The levels of BAX, TXNIP, MMP9, and TNF-α increased post-treatment while BCL-2 decreased. Control samples showed constant levels of pH and pro-apoptotic markers. The FFAs in the control samples were increased by 41.6%-51.4%.

Conclusion: The changes in the levels of the pro-apoptotic markers conformed to the previously reported elevated fat apoptosis post-HIFEM treatments. These effects were accompanied by an increase in FFA levels, and by reduced pH levels, due to the increased acidity in the adipose tissue. Further research is required to explore the potential of nonthermal induction of apoptosis.

KEYWORDS
apoptosis, ER stress, fat disruption, high-intensity focused electromagnetic field technology, non-thermal

1 | INTRODUCTION

Too many calories consumed versus too little energy expended due to low levels of physical activity is considered the main cause of fat accumulation, especially in the lower body,[1] resulting in an undesirable aesthetic appearance. In an effort to improve their aesthetic appearance, patients often attempt to reduce this excess fat by dietary restraint, lifestyle modification, or increased physical activity. However, achieving a sustainable fat reduction requires a considerable commitment and dedication, while the desired results take significant time to manifest. Patients often seek help through aesthetic medicine to help further bolster their effort.

Aesthetic medical procedures can yield a volumetric reduction of fat, either invasively through surgical removal of fat deposits or noninvasively by the elimination of cells forming the subcutaneous tissue—the adipocytes. The noninvasive elimination of fat occurs through the action of various physical, chemical, and biological factors, resulting in adipocyte necrosis or apoptosis.[2]

Fat necrosis is a pathological and unregulated process. Apoptosis, on the other hand, is a highly regulated physiological process where the affected cell actively destroys itself (programmed cell death).[3] The induction of an apoptotic response in fat cells above normal physiological levels has long been considered temperature-dependent only, achievable by the heating of subcutaneous tissue[4] or its cooling below the freezing point.[5] The effectiveness of such approaches has been investigated by multiple studies.[6-8]

Recently published research unveiled that it is also possible to achieve similar fat reduction through apoptosis of adipocytes in a nonthermal manner with the application of the High-Intensity Focused Electromagnetic field (HIFEM) technology.[9] This novel technology utilizes the principles of electromagnetic induction to depolarize motor neurons, thus stimulating intense involuntary muscle contractions, by bypassing the central nervous system. Such intense muscle recruitment/load appears to be able to trigger an exaggerated need for energy at the cellular level. This perceived extreme energy need, hormonally signaled by the muscle, then leads to the adipocytes dysfunction and consequently to apoptosis. A similar study by Weiss et al, conducted on a porcine animal model, showed objective histological data and increased levels of fat apoptosis accompanied by elevated concentrations of free fatty acids (FFA), creatine kinase, and various apoptotic markers in the blood plasma after the HIFEM treatment.[9] The authors proposed that stress of endoplasmic reticulum could have been the mechanism for the observed apoptotic acceleration.

Several additional studies demonstrated that increased levels of extracellular FFA have the potential to induce endoplasmic reticulum (ER) stress reaction.[10,11] The ER is a central cellular organelle responsible for lipid, glucose, and protein metabolism, and it is also highly responsive to cellular nutrient and energy status.[12] The efficient functioning of the ER is essential for cell survival. However, ER is highly sensitive to stresses that perturb cellular energy levels. Such stress reduces the protein folding capacity of this organelle, which results in the accumulation and aggregation of unfolded proteins, referred to as ER stress. The cells themselves have developed various protective strategies to resist the deleterious effect of ER stress, referred to as an unfolded protein response (UPR). Nonetheless, when protein aggregation cannot be resolved through a cellular reparative processes, the pro-survival signaling mechanisms alter the pro-apoptotic and ER stress responses ultimately leading to apoptotic cell death.[12]

This study aims to build on the previous research, providing further evidence of increased apoptotic levels post-HIFEM treatments.[9] The proposed mechanism of adipocyte apoptosis is based on ER stress through the overflow of FFA, though previously no study measured the FFA levels directly in the treated tissue. A primary goal of this study is to further investigate the underlying mechanism of nonthermal apoptotic effect of the HIFEM procedure. Assessing the levels of FFA and ER stress markers in the porcine fat tissue should bring valuable insight into the nature of this process and provide supportive or refuting evidence for the proposed ER-stress-based mechanism of apoptosis.

2 | MATERIALS AND METHODS

The study protocol was approved by the institutional review board (IRB) of The Ministry of Agriculture of the Czech Republic, which also supervised the experiment.

2.1 | Description of animal model

Two Large White pigs (approximately 1 year old, 80-90 kg of weight) were used for the experiment. The pigs were clinically examined during the recruitment phase to ensure only those in the proper health conditions were recruited. A 1-week acclimation period was established for stabilization of the animals in the new environment. Prior to treatment, animals received anesthesia, dosed by a veterinarian who supervised the procedure, to minimize any pain or discomfort to the animals during the treatment and biopsy sampling. The general anesthesia was achieved by inhalation of anesthetic agents (tiletamine 2 mg/kg; zolazepam 2 mg/kg; ketamine 2 mg/kg; xylazine 2 mg/kg); thereafter, it was sustained by the intravenous continuous influx of 2% propofol (1-2 mg/kg) through a cannula inserted into a vein in the pig's ear. Both animals were intubated to prevent respiratory arrest.

2.2 | Treatment procedure

Both animals underwent one 30-minute treatment of the thigh with the investigated device (EMSCULPT; BTL Industries Inc), utilizing HIFEM technology. The circular coil, located at the distal end of the

device's applicator, generates alternating dynamic magnetic fields of intensities of up to 1.8 Tesla. During the treatment, the device's applicator was attached to the animal's thigh, secured by a fixation belt. The intensity of the stimulus was set to 100% of the device's possible output.

After the completion of the experiment, the studied animals were painlessly euthanized while under general anesthesia (described earlier) through the injection of an approved and certified veterinary euthanasia drug (T-61; dosed according to the instructions of the manufacturer).

2.3 | Collection of biopsy specimen

In total, five punch biopsies (6 mm in diameter) containing subcutaneous tissue with the adjacent skin tissue were obtained from each pig and prepared for evaluation. Three biopsies were obtained from the treated region, and two were taken from a nontreated abdominal area, which served as a control (taken immediately after treatment and then again after 8 hours). The biopsies were preserved for further analysis in an RNA solution, required for PCR analysis and deep freezing for detection of FFA.

2.4 | pH meter analysis

Local pH in subcutaneous tissue was measured in vivo by GRYF 259 digital-microprocessor pH meter (GRYF HB) with combined electrode FC430B (Hanna Instruments). The device was calibrated before each session. The pH measurements involved the insertion of the pH electrode into the wound. To minimize tissue traumatization, measurements (N = 3) were performed only once at each biopsy site. The pH was obtained at baseline, immediately after, and 8 hours post-treatment to document any fluctuation above/below its physiological baseline levels.

2.5 | RNA markers expression

The relative expression of apoptotic biomarkers in the taken samples of tissue was investigated to document hypothesized stress reaction. At the beginning of this procedure, the total RNA was isolated using the Tri RT Reagent (MRC) and purified in the RNeasy Mini Kit columns (Qiagen). The purity of RNA was expressed as the ratio of absorbances at 260 and 280 nm. M-MLV reverse transcriptase and oligo (dT) primer specific mRNA were used for cDNA generation. The expression of five genes of interest that are involved in ER stress apoptotic processes (TNF-α, MMP9, BAX, TXNIP, and BCL-2) was calculated relative to the expression of the reference gene TBP1,[13] which was chosen as stably expressed using the NormFinder algorithm (2004, Aarhus University Hospital). A qPCR analysis was performed on a LightCycler 480 device (Roche) using QIAGEN QuantiTect SYBR Green PCR MasterMix (Qiagen). Polymerase Chain Reaction plates were automatically filled by the Nanodrop II liquid dispensing robot (BioNex Solutions Inc). Gene-specific primers were partly adopted or designed using the NCBI primer designing software Primer-BLAST (see Table 1). The chain reactions were triplicated and were run under the following conditions: denaturation at 95°C for 15 minutes and 50 amplification cycles at 95°C for 15 seconds, followed by 58°C for 30 seconds and 72°C for 30 seconds. A melt curve analysis using the LightCycler 480 software (Roche Molecular Systems Inc; version 1.5.0.39) was performed to test the specificity of PCR products. A 10-fold serial dilution of DNA template was used to create a standard curve. Amplification efficiency (E) of each primer set was determined, and since the E-values fluctuated in the range from 1.892 to 2.245, an optimal efficiency of 2.0 was used to calculate the gene expression.

2.6 | FFA quantification

The total amount of FFA released from adipocytes was examined. The examination included (but was not specific to) palmitic acid, palmitoleic acid, stearic acid, oleic acid, and arachidonic acid. First, adipose tissue samples (approx 0.2 g) were homogenized in methanol. Nonpolar lipids, together with FFA, were extracted into a nonpolar solvent from a weakly acidic environment. The separation of FFA from co-extruded nonpolar lipids was performed by normal-phase liquid chromatography. A triple quadrupole mass spectrometer was used to detect mass spectra of ionized FFA. Its ionization was performed by an atmospheric pressure photoionization method (APPI). From the resulting relative intensities of the ions in mass spectra, we calculated areas under the peaks related to FFAs, which referred to the total amount in the studied specimens.

2.7 | Macroscopic analysis

Any signs of observable side effects or adverse events (bruising, redness or changes of skin texture) caused by treatment were immediately addressed after the therapy and during the housing. Also, any changes in behavioral pattern, gait, or movement stereotypes were monitored by the veterinarian.

2.8 | Statistical analysis

The results are expressed as mean ± standard deviation (SD). The levels of pH before and after the treatment were statistically evaluated. Analysis was performed using two-tailed Wilcoxon signed-rank test (α = 0.05) to identify any significant difference between means of dependent samples.

Gene Acc. No[a]	5′- Forward primer- 3′ 5′- Reverse primer- 3′	Product length[b]/E[c]/ characterization of gene
TNF-α NM_214022.1	CCCCCAGAAGGAAGAGTTTC CGGGCTTATCTGAGGTTTGA	92/2.079/Pro-apoptotic
MMP9 NM_001038004.1	CCTTGAACACACACGACATCTTC CCACATAGTCCACCTGATTCACC	111/1.971/Pro-apoptotic
BAX XM_003127290.5	AACATGGAGCTGCAGAGGATG GTTGCCGTCAGCAAACATTTC	96/1.956/Pro-apoptotic
TXNIP NM_001044614.2	GATGACACAGATGGCTCTCAAGAC GGATGCAGGGATCACCTCAC	99/1.925/Pro-apoptotic
BCL-2 XM_021099593.1	AGTACCTGAACCGGCACCTG CAGCCAGGAGAAATCAAATAGAGG	110/1.892/Anti-apoptotic

[a]Accession number in GenBank National Center for Biotechnology Information (NCBI).
[b]Size of the PCR product of adopted primers was derived using Primer-BLAST software based on the current nucleotide sequences available in the NCBI GenBank.
[c]Efficiency of specific primer set.

3 | RESULTS

3.1 | General observations

The animals were in good condition during the acclimation phase, as well as after the treatment procedure. We observed no side effects or adverse events while the treated area demonstrated no visible erythematous cutaneous reaction to the HIFEM application.

3.2 | pH levels

The average pH of the treated area at baseline (7.30 ± 0.12) corresponded to normal physiological values and did not differ from the measurements at the control site. Immediately after the treatment, pH significantly decreased by 0.70 points on average ($P = .001$), showing a slightly acidic value of 6.60 ± 0.07. The control measurements demonstrated a similar pattern but to a lesser extent. Although the pH mildly and insignificantly decreased, still it remained at near levels, indicating a more natural environment (7.11 ± 0.11). After 8 hours, pH levels returned back to nearly the original baseline levels (see Figure 1).

3.3 | RNA markers

The results of PCR analysis are summarized in Table 2. The relative expression of the examined genes show to be more upregulated (TNF-α, MMP-9, BAX, TXNIP) rather than downregulated (BCL-2) in response to the external stimulus delivered by the HIFEM fields. Conversely, the control samples did not manifest any significant fluctuations among the examined markers, and their expression immediately post-treatment and 8 hours post-treatment was comparable to the baseline.

In general, we observed a greater response in the levels of studied markers at 8 hours post-treatment. The highest fold change was observed in the TNF-α (2.14-fold increase) followed by TXNIP (2.01-fold increase) and MMP9 (1.62-fold increase). Conversely, the BAX marker reached its maximum immediately after treatment (1.43-fold change), while the BCL-2 production was attenuated by 26% in comparison with the baseline.

3.4 | FFA total amount

The assessment of free fatty acids demonstrated a dramatic variation in time, which coincided with the pH measurements (see Figure 2). The post-treatment biopsies of the treated tissue showed significantly increased levels of FFA's, by 127.10%, while control samples demonstrated change to a lesser extent, with FFA levels equal to 41.60%. Moreover, the FFA overflow showed to be sustained even 8 hours post-treatment, reaching an increment change of 134.10% in treated samples and 51.40% in the control samples when compared to baseline.

4 | DISCUSSION

One of the major finding of our study was the documented evidence of elevated levels of FFA in subcutaneous tissue after single HIFEM treatment. The release of FFA was followed by a decrease in pH levels and was accompanied by considerable fluctuations in the expression of important apoptotic markers, such as TNF-α, MMP9, TXNIP, BAX, and BCL-2. The presence of FFA was confirmed and proven by mass spectrometry analysis and a transient increase of acidity in subcutaneous tissue.

The levels of FFA and the pH values measured immediately after the treatment followed a similar complementary trend. As a result of dramatic lipid breakdown, FFAs were released and consequently caused a decrease of the physiological pH levels to slightly acidic

FIGURE 1 Results of pH
measurements in subcutaneous tissue
(mean ± SD) at baseline, immediately
after treatment (after Tx), and 8 h after
treatment (after 8 h). The statistically
significant difference (P = .001) between
baseline and post-treatment measures is
depicted by an asterisk (*)
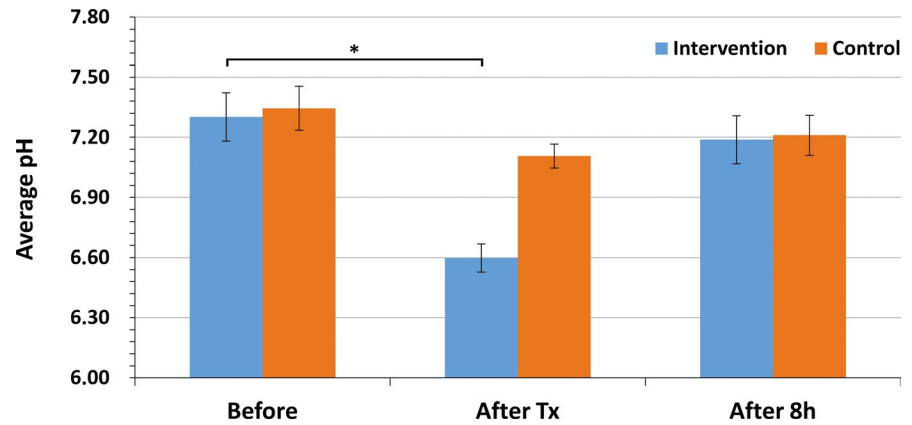
values. Although the levels of FFA remained highly elevated 8 hours post-treatment, the pH returned close to its original values, as the body seeks to restore itself to a more neutral pH to protect the internal cellular environment.

The control samples also showed increased FFA levels in post-treatment measurements and followed the same linear relationship, as the samples taken from the treatment site, although not to the same extent. We hypothesize that it is due to the complexity of the response to the HIFEM treatment. The initiation of triglyceride breakdown into FFA, triggered by intense muscle activity, is often linked to the hormonal release of epinephrine into the bloodstream.[14] Due to bloodstream transport, the epinephrine cannot be selectively delivered to only the localized treatment area, but creates more of a systemic response. This helps to explain the increase in FFA levels in the control area, though not high enough to trigger adipocytes apoptosis. This was also documented by the nonchanged RNA markers in the control area.

It has also been shown that elevated levels of FFA may trigger ER stress apoptotic pathways.[9-11,15] In our study, we observed considerable upregulation of studied ER stress markers in the treated animals, indicating a severe stress reaction. Similar to our findings, it was previously evidenced that during the ER stress in adipose tissue, the TNF-α mRNA expression is increased as the adipocytes enter the mechanism of programmed cell death.[16] In addition, Bouloumilé et al[17] documented that MMP9 could also be a key regulator of adipocytes differentiation, in terms of inhibition of adipose tissue growth. Based on the results of the qPCR analysis, the application of the HIFEM treatment resulted in upregulation of MMP9, indicating the possible contribution to ER stress in the treated adipose tissue.

The BAX is also a factor. It is a member of the BCL-2 family of proteins, and it exhibits pro-apoptotic activity. In resting conditions, BAX is kept inactive by its interaction with anti-apoptotic BCL-2. When severe stress of the ER occurs, the anti-apoptotic effect of the BCL-2 protein is eliminated, and its expression is blocked. This allows the activation of BAX, which leads to the initiation of ER-stress-induced apoptosis.[18] The following patterns have indeed been observed in our study when the BAX levels were upregulated while the BCL-2 levels were considerably decreased.

Furthermore, recent studies have demonstrated that TXNIP upregulation coincides with ER stress and can be induced at the transcriptional and post-transcriptional levels.[19,20] Our results revealed a gradually increasing expression of TXNIP reaching 2.01-fold at the 8 hours post-treatment, which implies an upcoming apoptotic change in the adipose tissue.

The first documented evidence of HIFEM-induced adipocyte apoptosis was recently performed by Weiss et al[9] in a porcine animal model. In addition to the evaluation of RNA markers, they also examined various recognized blood parameters related to both fat and muscle metabolism. One of the major contributions of this study is that it further describes the association between intense muscle load induced by supramaximal contraction and the subsequent stress reaction of the adjacent adipose tissue, caused by the increased levels of FFA. It has been shown that such extensive muscle load resulted in an increased catalytic activity of lactate dehydrogenase (LDH) and creatinine kinase (CK) 8 hours post-treatment. Although their qPCR values are not equally comparable to ours, due to the different reference gene chosen (HPRT1), the observed results revealed similar tendencies. In response to the excessive overflow of FFA measured

TABLE 2 Relative expression of studied apoptotic biomarkers including control samples (C) at baseline, immediately after treatment (after Tx) and 8 h after treatment (after 8 h)

Sampling	TNF-α	MMP-9	BAX	TXNIP	BCL-2
Before	0.050 ± 0.002	0.088 ± 0.023	0.12 ± 0.01	28.89 ± 1.36	0.54 ± 0.13
After Tx	0.052 ± 0.001	0.083 ± 0.022	0.17 ± 0.01	35.43 ± 2.05	0.42 ± 0.07
After 8 h	0.107 ± 0.002	0.142 ± 0.027	0.14 ± 0.02	58.08 ± 8.50	0.40 ± 0.08
After Tx (C)	0.057 ± 0.007	0.081 ± 0.017	0.13 ± 0.02	24.31 ± 6.46	0.52 ± 0.07
After 8 h (C)	0.053 ± 0.003	0.083 ± 0.035	0.13 ± 0.01	26.07 ± 5.14	0.49 ± 0.10
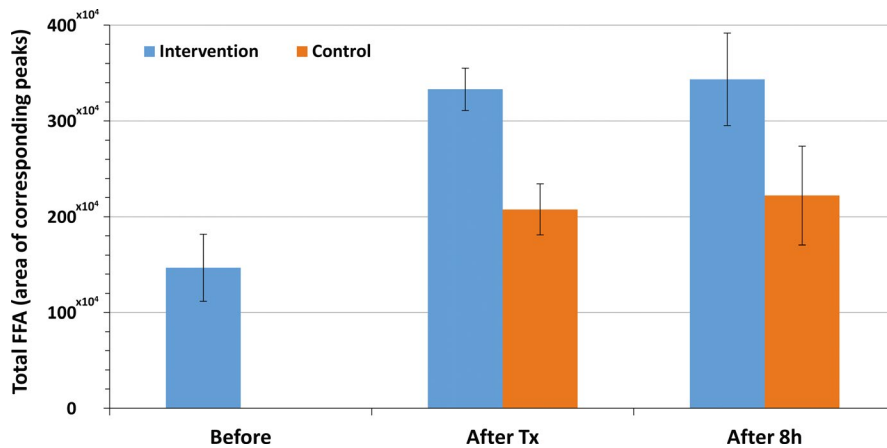
FIGURE 2 Results of total FFA amount in specimens (mean ± SD) at baseline, immediately after treatment (after Tx), and 8 h after treatment (after 8 h). Values correspond to the overall area under the peaks obtained by mass spectrometry

in the bloodstream right after the HIFEM application, the fat biopsies showed a strong pro-apoptotic reaction, as indicated by (but not limited to) the upregulated expression of TNF-α and MMP9, accompanied by a documented decrease in the levels of BCL-2. Examination of apoptotic markers and blood plasma was also complemented with the TUNEL analysis which showed an elevation of apoptotic index (ratio of apoptotic cells in the specimens) up to 35.95% at 8 hours after the treatment.

High-Intensity Focused Electromagnetic technology has proven itself to be safe. There were no adverse events, such as erythema, no change in epidermal/dermal integrity, or changed behavioral patterns in the treated animals. This observation is in line with previous research,[9,21,22] as no adverse events were reported in any of the previous studies.

This study provides novel findings that support the previously documented induction of ER stress apoptosis in subcutaneous tissue. Our investigation benefited from three different quantitative methods of evaluation, accompanied by control site measurements, utilized to further verify a link between the increased concentration of FFA and fat apoptosis.

Conversely, we are aware that these evaluation methods do come with limitations. One of the shortcomings is a relatively small sample size of only two animals, which did not allow us to perform a robust statistical analysis. Additionally, due to the short-term nature of studied treatments, we established the length of the follow-up examination up to 8 hours. This timeframe was similar to the previous study by Weiss et al[9] In future, a higher number of data points should be used, with an increased period of follow-up to determine and further understand the dynamics of this investigated phenomenon. Finally, we also need to consider that although the results of qPCR analysis coincided with the previous findings, the association between levels of BAX and BCL-2 might be a subject for a more detailed investigation. Also, the use of a porcine model, instead of a human trial, could be considered a limitation. Porcine models are widely recognized as an acceptable model for studies investigating digestion, diet, and fat metabolism, due to its similarities in gastro-intestinal tract, organ-size, genetics, dietary habits, and metabolism.[23-25] Due to the high similarity with humans, porcine subcutaneous fat is even often used as a model for studying RNA of subcutaneous adipose tissue.[26]

5 | CONCLUSION

Results of this animal study support the previously published findings, stating that HIFEM-induced contractions evoke a strong metabolic reaction, which can trigger a cascade effect resulting in FFA oversaturation. This rapid elevation of FFA levels appears to lead to the apoptosis of adipocytes, mediated through an endoplasmic reticulum stress reaction. We fully recognize, this studied phenomenon may not be the only mechanism involved and that other factors may play a role as well. Further research should be conducted to provide additional evidence and to test other hypotheses as well, as it is possible the outcome is a result of several other biochemical processes. Our research is only another piece into the puzzle which needs to be resolved, but our findings strongly indicate that FFA overflow plays significant a role.

CONFLICT OF INTEREST
Dr Bernardy and Dr Halaas have nothing to disclose.

ETHICAL APPROVAL
This prospective animal study was approved by the Institutional Animal Care and Use Committee (IACUC). The procedures were carried out according to the Good Laboratory Practices (GLP) standards, and animal care complied with the convention for the protection of vertebrate animals.

ORCID
Yael Halaas 🆔 https://orcid.org/0000-0001-6550-9316

REFERENCES
1. Jensen MD. Role of body fat distribution and the metabolic complications of obesity. *J Clin Endocrinol Metab.* 2008;93(11 Suppl 1):S57-S63.
2. Alizadeh Z, Halabchi F, Mazaheri R, Abolhasani M, Tabesh M. Review of the mechanisms and effects of noninvasive body contouring

devices on cellulite and subcutaneous fat. *Int J Endocrinol Metab.* 2016;14(4):e36727.

3. Gordeziani M, Adamia G, Khatisashvili G, Gigolashvili G. Programmed cell self-liquidation (apoptosis). *Ann Agrar Sci.* 2017;15(1):148-154.

4. Yanina I, Orlova TG, Tuchin V, Altshuler G. The morphology of apoptosis and necrosis of fat cells after photodynamic treatment at a constant temperature in vitro. *Prog Biomed Opt Imaging Proc SPIE.* 2011;7887:78870X.

5. Nassab R. The evidence behind noninvasive body contouring devices. *Aesthet Surg J.* 2015;35(3):279-293.

6. Zelickson B, Egbert BM, Preciado J, et al. Cryolipolysis for noninvasive fat cell destruction: initial results from a pig model. *Dermatol Surg.* 2009;35(10):1462-1470.

7. McDaniel D, Lozanova P. Human adipocyte apoptosis immediately following high frequency focused field radio frequency: case study. *J Drugs Dermatol.* 2015;14(6):622-623.

8. Mulholland RS. Non-surgical body contouring: introduction of a new non-invasive device for long-term localized fat reduction and cellulite improvement using controlled, suction coupled, radiofrequency heating and high voltage ultra-short electrical pulses. *J Clin Exp Dermatol.* 2012;03(04):157.

9. Weiss RA, Bernardy J. Induction of fat apoptosis by a non-thermal device: mechanism of action of non-invasive high-intensity electromagnetic technology in a porcine model. *Lasers Surg Med.* 2018;51(1):47-53.

10. Jiao P, Ma J, Feng B, et al. FFA-induced adipocyte inflammation and insulin resistance: involvement of ER stress and IKKβ pathways. *Obesity.* 2011;19(3):483-491.

11. Cnop M, Foufelle F, Velloso LA. Endoplasmic reticulum stress, obesity and diabetes. *Trends Mol Med.* 2012;18(1):59-68.

12. Hummasti S, Hotamisligil GS. Endoplasmic reticulum stress and inflammation in obesity and diabetes. *Circ Res.* 2010;107(5):579-591.

13. Zelnickova P, Leva L, Stepanova H, Kovaru F, Faldyna M. Age-dependent changes of proinflammatory cytokine production by porcine peripheral blood phagocytes. *Vet Immunol Immunopathol.* 2008;124(3-4):367-378.

14. Horowitz JF, Klein S. Lipid metabolism during endurance exercise. *Am J Clin Nutr.* 2000;72(2 Suppl):558S-563S.

15. Hardy S, El-Assaad W, Przybytkowski E, Joly E, Prentki M, Langelier Y. Saturated fatty acid-induced apoptosis in MDA-MB-231 breast cancer cells. A role for cardiolipin. *J Biol Chem.* 2003;278(34):31861-31870.

16. Khan S, Wang CH. ER stress in adipocytes and insulin resistance: mechanisms and significance (Review). *Mol Med Rep.* 2014;10(5):2234-2240.

17. Bouloumié A, Sengenès C, Portolan G, Galitzky J, Lafontan M. Adipocyte produces matrix metalloproteinases 2 and 9: involvement in adipose differentiation. *Diabetes.* 2001;50(9):2080-2086.

18. Szegezdi E, Logue SE, Gorman AM, Samali A. Mediators of endoplasmic reticulum stress-induced apoptosis. *EMBO Rep.* 2006;7(9):880-885.

19. Lerner AG, Upton JP, Praveen PVK, et al. IRE1α induces thioredoxin-interacting protein to activate the NLRP3 inflammasome and promote programmed cell death under irremediable ER stress. *Cell Metab.* 2012;16(2):250-264.

20. Oslowski CM, Hara T, O'Sullivan-Murphy B, et al. Thioredoxin-interacting protein mediates ER stress-induced β cell death through initiation of the inflammasome. *Cell Metab.* 2012;16(2):265-273.

21. Kinney BM, Lozanova P. High intensity focused electromagnetic therapy evaluated by magnetic resonance imaging: safety and efficacy study of a dual tissue effect based non-invasive abdominal body shaping: MRI evaluation of electromagnetic therapy. *Lasers Surg Med.* 2019;51(1):40-46.

22. Katz B, Bard R, Goldfarb R, Shiloh A, Kenolova D. Ultrasound assessment of subcutaneous abdominal fat thickness after treatments with a high-intensity focused electromagnetic field device: a multicenter study. *Dermatol Surg.* 2019;45(12):1542-1548.

23. Groenen MAM, Archibald AL, Uenishi H, et al. Analyses of pig genomes provide insight into porcine demography and evolution. *Nature.* 2012;491(7424):393-398.

24. Spurlock ME, Gabler NK. The development of porcine models of obesity and the metabolic syndrome. *J Nutr.* 2008;138(2):397-402.

25. Nielsen KL, Hartvigsen ML, Hedemann MS, Lærke HN, Hermansen K, Bach Knudsen KE. Similar metabolic responses in pigs and humans to breads with different contents and compositions of dietary fibers: a metabolomics study. *Am J Clin Nutr.* 2014;99(4):941-949.

26. Mentzel CMJ, Anthon C, Jacobsen MJ, et al. Gender and obesity specific microrna expression in adipose tissue from lean and obese pigs. *PLoS ONE.* 2015;10(7):e0131650.